Macromolecular Research, Vol. 10, No. 6, pp 345-358 (2002)

Novel Smart Polymeric Composites for Thermistors and Electromagnetic Wave Shielding Effectiveness from TiC Loaded Styrene-Butadiene Rubber

Yong Kiel Sung*

Department of Chemistry, College of Science, Dongguk University, Seoul 100-715, Korea

Farid El-Tantawy

Department of Physics, Faculty of Science, Suez Canal University, Ismailia, Egypt

Received Oct. 10, 2002; Revised Dec. 6, 2002

Abstract: The electrical conductivity during vulcanization process was measured as a function of time for the system of TiC loaded styrene-butadiene rubber (SBR) composites. The phenomenon of negative and positive temperature coefficients of conductivity and its conduction mechanism were also studied for the SBR polymeric composites. The current-voltage characteristics of the polymeric composites were non-linear in high voltage and showed a switching effect. The effects of temperature on the thermal conductivity and effective dielectric constant were measured. The measured parameters were found to be dependent on TiC concentration. The electromagnetic wave shielding (EMS) of the SBR-TiC polymeric composite was also examined. The SBR filled with TiC could be expected to be promising novel smart polymeric composites for self-electrical heating, temperature sensor, time delay switching, and electromagnetic wave shielding effectiveness.

Keywords: SBR-TiC polymeric composites, thermistor, electrical conductivity, electromagnetic wave shielding effectiveness.

Introduction

There has been recently rapid development of polymer heating devices with long lifetime and high efficiency.[1,2] The knowledge of thermal properties such as heat capacity, heat transfer, and thermal conductivity is fundamental to every application in polymer science and technology. That will contribute much to the understanding of the thermal equilibrium process and hence to optimize operation conditions.[3] The electrical conductivity has been generally shown to depend on the nature of the polymer, filler, and filler matrix interactions. The processing technique is the key factor in the determination of the physical properties. TiC is one of important materials for high temperature applications because of its high melting point, hardness, elastic modulus, and electrical conductivity, relatively low coefficient of thermal expansion, and non-polar like carbon black.[4] Carbon black is unquestionably the most widely used reinforcing filler in polymer formulations, owing to the physico-chemical characteristics and performances it gives to cured rubbers. Carbon black filled composites have wide applications, such as heater[2,3] flooring materials to dissipate static electric charge,[1,4] pressure sensitive sensors that can be used for shockproof switches,[2,5] sensors for measurement of vehicle weight to collect toll tax on roads,[6] resistor,[7] electromagnetic radiation shielding,[8,9] temperature sensing,[1,2,10] and compensation. The smartness of this kind of composites can be distinguished by the double negative and positive temperature coefficient of conductivity (NTCC and PTCC) effects. Therefore, the development of NTCC and PTCC effects of polymer composites can be considered as one of the major advances in electronic materials research.

In the present study, the main target of this work is to present for the first time the effect of TiC as conducting and reinforcing filler on the vulcanization reaction, electrical, thermal, and electromagnetic wave shielding properties of SBR polymeric composites, aiming to understand the physico-chemical properties of these new composites for consumer products as NTCC/PTCC thermistors and electromagnetic wave shielding effective materials.

Experimental

Materials and Characterization. Elastomer selected for the present study is a commercial grade SBR-1502(Good-

*e-mail : yksung@dongguk.edu

year, USA). SBR with various ingredients used in this work were prepared according to the recipes given in Table I. A commercially grade of titanate LIC A 12 of Kenrich Petrochemicals was used as a coupling agent. Mixing and/or compounding of different TiC (particle size 5 μm) was carried out following the conventional technique in a two roll mill 170 mm diameter, working distance 300 mm, speed of 18 rpm and gear ratio 1.33 at a temperature of 50 °C. An overall mixing time of 5 hrs at 50 °C was allowed to ensure uniform and efficient dispersion of conductive particles in the elastomer matrix. The vulcanization and curing of the rubber compounds were carried out in an electrically heated press between stainless steel plates at 150 °C and pressure 500 kPa for dwelling time 10 hrs. The samples of diameter 1 cm and thickness 0.5 cm were prepared by molding. Thin brass electrode was embedded into samples during vulcanization process to minimize the contact resistance.[2] The electrical conductivity (σ) of the sample was recorded with time during vulcanization. The details of the experimental set-up have been recently reported elsewhere.[2] The conductivity was measured in dry air at room temperature with a Keithley - 412 Pico meter/voltage source with a desirable basic program. The vulcanization fraction (VF) was determined by soaking the test samples in kerosene for 30 hrs, after which the samples were dried to a constant weight in vacuum at 50 °C.

The insoluble fraction was calculated as the ratio of mass loss and initial mass by using this equation:[11, 12]

$$(VF)\ \% = \left(\frac{\omega_1}{\omega_0}\right) \times 100 \tag{1}$$

where, ω_1 is the weight of insoluble portion of the sample, and ω_0 is the weight of initial sample.

The volume fraction of SBR rubber (V_r) was calculated according to the equation:[13]

$$\left(\frac{1}{V_r}\right) = 1 + \left(\frac{\omega_s \rho_r}{\omega_0 \rho_s}\right) \tag{2}$$

where, ω_s is the weight of absorbed solvent, ρ_s and ρ_r are the densities of the solvent and SBR compound, respectively. Average molecular weight between cross-links can be determined by Flory-Rehner equation:[14]

$$M_c = \frac{(\rho_r V_k)(DS_E^{-1/3} - 1/2DS_E^{-1})}{\ln(1 - DS_E^{-1}) + DS_E^{-1} + \chi DS_E^{-1}} \tag{3}$$

where V_k is the molar volume of kerosene. DS_E is the equilibrium degree of swelling and is given as:[15]

$$DS_E = 1 + \left(\frac{\rho_r}{\rho_s}\right)\left(\frac{\omega_2}{\omega_0 - 1}\right) \tag{4}$$

where ω_2 is the weight of sample after swelling in kerosene for 2 days.

The polymer-solvent interaction parameter χ was calculated from the values of DS_E at temperature (20 °C) using the equation:[16]

$$\chi = 0.431 - 0.311 DS_E^{-1} - 0.036 DS_E^{-2} \tag{5}$$

According to the affine and phantom network models the molecular weight between physical cross-links is given by the following equation.[17]

$$M_c(affine) = \frac{(\rho_r V_k V_r)\left(1 - \frac{\mu}{\phi} V_r^{\frac{1}{3}}\right)}{-(\ln(1 - V_r) + V_r + \chi V_r^2)} \tag{6}$$

$$M_c(phantom) = \frac{(\rho_r V_k V_r)\left(1 - \frac{2}{\theta}\right)}{-(\ln(1 - V_r) + V_r + \chi V_r^2)} \tag{7}$$

where μ is the number of effective network chains/cm^3 of crosslinked polymer (chain density and/or network density, θ is the junctions functionality or number of chains emanating from each crosslink (usually assumed to be 4), and ϕ is the

Table I. The Formulation of the Recipes

Ingredients	FT0	FT5	FT10	FT15	FT20
SBR-1502	100	100	100	100	100
Pb-stearate	5	5	5	5	5
Zinc oxide	5	5	5	5	5
Naphthenic oil	10	10	10	10	10
TMTD[a]	1	1	1	1	1
CBS[b]	1.5	1.5	1.5	1.5	1.5
PβN[c]	1	1	1	1	1
Styrenated phenol	1	1	1	1	1
Sulfur (S)	1	1	1	1	1
Ti- LICA 12[d]	1	1	1	1	1
TiC	**50**	**55**	**60**	**65**	**70**

[a]Tetramethylthiuranm disulfide. [b]*N*-cyclohexylbenzthiazyl sulphenamide. [c]Phenyl - β naphthylamine. [d]Titanate coupling agent.

number of junction given as: $\phi = 1 - 2/\theta$.

The crosslinking density (CLD) is determined by the following equation:[18]

$$(CLD) = \left(\frac{\rho_r N_A}{M_c}\right) \tag{8}$$

where N_A is Avogadro's number. The extent of TiC reinforcement(γ) on SBR polymeric composites can be determined as: [19]

$$\left(\frac{V_r}{V_{r0}}\right) = 1 - \gamma\left(\frac{\Phi}{1-\Phi}\right) \tag{9}$$

where V_{r0} and V_r are the initial and final volume fractions of rubber in the composites. Φ is the content of TiC.

The interparticle distance (IPD) between conductive aggregates is given by the following equation.[20]

$$(IPD) = d\left[\left(\frac{k\pi}{6V_r}\right)^{1/3} - 1\right] \tag{10}$$

where d is the SBR particle diameter and $k = 1$ for cubic packing. The thermal conductivity (λ) was measured by the thermal in flash techniques. Specific heat (C_p) of the sample was carried out with a differential scanning calorimeter (Perkin Elmer DSC-2) using sapphire as the reference material. The thermal diffusivity (δ) are calculated by the equation:[20]

$$\delta = \frac{\lambda}{\rho_r C_p} \tag{11}$$

Dielectric constant at various temperatures has been estimated via Hewlett-Packard impedance analyzer. The effective dielectric constant (ε_{eff}) was calculated according to the following equation.[20]

$$\varepsilon_{eff} = \frac{\varepsilon}{(1-V_r)^3} \tag{12}$$

where ε is the dielectric constant of polymer composites. Thermoelectric power (TEP) measurements were carried out by a standard technique in air atmosphere.[2] Morphology study of the SBR polymeric composite was conducted on scanning electron microscopy (SEM, JEOL). Hardness (H_v) has been determined using a universal testing machine (ASTM-D 2240-78). The surface energy (SE) was measured by surface tensiometer (GBYO-A3, Japan). Viscosity(η) was measured by viscometer (VM-1A, Japan). From this data we calculated the charge carriers mobility and the number of charge carriers by the following equation.[21]

$$n = \frac{BI_H}{qhV_H} \tag{13}$$

where B is the applied magnetic field, q is the charge per one charge carrier, h is the sample thickness; I_H and V_H are the Hall current and voltage, respectively.

Results and Discussion

Vulcanization and Network Structure. The crosslinking of SBR polymeric composites was carried out using S and titanate as a double crosslinking agent in the presence of TMTD at 150 °C and 500 kPa. The electrical conductivity versus time during vulcanization process of SBR composites with different content of TiC is depicted in Figure 1. It can be seen that the vulcanization process shows a S-shaped profile. With increasing TiC content the S-shaped shifts to shorter time scales. The higher conductivity level (i.e. at the beginning of curing) is probably due to better packing characteristics in the green stage, which induces the driving force of curing process.[2] It is also possible that TiC acts as a catalyst and the molecular architecture of SBR polymeric matrix was affected during mastication process.[1] However, the behavior of vulcanization process in Figure 1 can be divided into two stages: first stage (I), the electrical conductivity depends on TiC content which is attributed to ordering of conductive sites and thermal activation causing rapid crosslinking density.[1,2,22] In this stage, the relative size of the network increases till all of the aggregated chains are linked by covalent bonds. Hence, the covalent bonds are established between chains and a three-dimensional network is progressively formed.[1,23] It is suggested that the TiC reacted with active sites of SBR. The active sites would assist and facilitate the mobilization of the charge carriers and hence cause an increase in the conductivity. In addition, the interaction between conductive particles and active sites of SBR rubber helps to create carriers (i.e. TiC acts as carriers reservoir and/or pinning center effect), and to improve the conducting properties of polymers. In the second stage (II), the conductivity remains steady at long time for about 20 hrs; this plateau

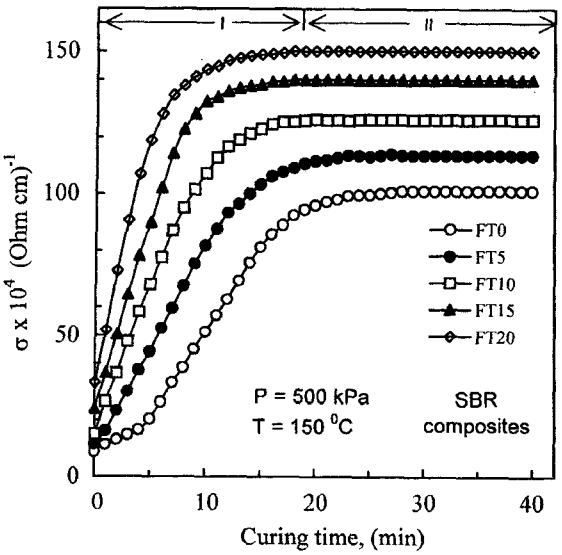

Figure 1. The electrical conductivity versus time during vulcanization process of SBR composites with different content of TiC.

indicating the completion of vulcanization reaction and the crosslinking reactions results only in an increase of the network density. We speculate that in this stage the inter-particle distance between conductive phases decreases and aggregate conductivity is relatively insensitive to TiC concentrations due to the formation of extra crosslinks introduced through TiC itself.

However, from Figure 1, the characteristic time constant (τ) during vulcanization process as a function of TiC content can be estimated by the empirical formula:

$$\left(\frac{\sigma-\sigma_0}{\sigma_m-\sigma_0}\right)=\left(1-e^{-\frac{t}{\tau}}\right) \tag{14}$$

where σ_m and σ_0 are the maximum and initial conductivity of the tested samples, respectively, and τ is the characteristic time constant depending on TiC content and was determined at $t = \tau$. The values of τ and VF against TiC content are depicted in Figure 2. It is seen that the τ decreases while the VF increases with TiC content. This is due to that TiC interacts with polymeric matrix and accelerates the driving force of vulcanization reactions (i.e. acts as an extender crosslinkers) and increases interlinks between conductive particles. The variations of H_v and V_r with TiC content for SBR composites are plotted in Figure 2. It is seen that the H_v and V_r increase with TiC content, which indicates the increase of the interfacial bond of rubber matrix and improve of the network structure core due to the reduction in the creep of rubber matrix during vulcanization as revealed by SEM analyses latter.[23] In addition, Figures 2 and 3 give the variation of IPD and γ versus TiC contents, respectively. From the plot, we observed an increasing of γ and decreasing of IPD as TiC contents increased. Figure 3 gives the variation of χ and DS_E versus TiC content. It is seen that χ and DS_E decrease with increasing TiC content. also increases while η decreases with increasing TiC content as shown in Figure 3. These results also support the TiC improves the domain connectivity and interface of rubber matrix. In more confirmation, Figure 4 shows the M_c, M_{affine}, $M_{phantom}$ and CLD against TiC content. It is clear that M_c decreases while CLD increases with TiC concentration. The higher crosslink densities may be attributed to the better interaction between

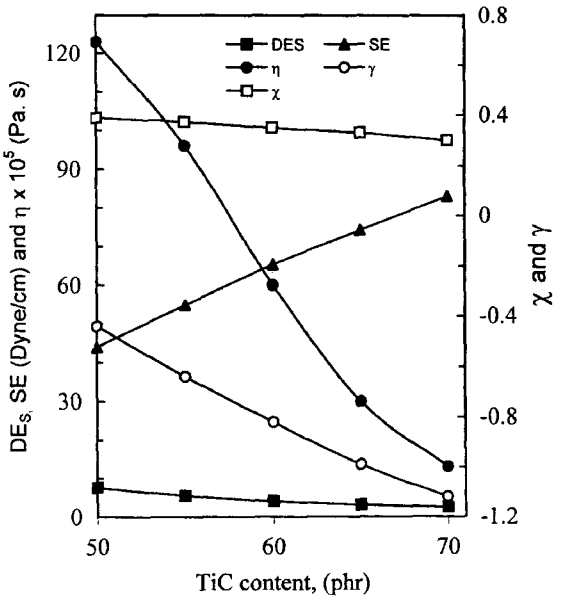

Figure 3. Variation of γ, χ, DS_E, SE and η versus TiC content.

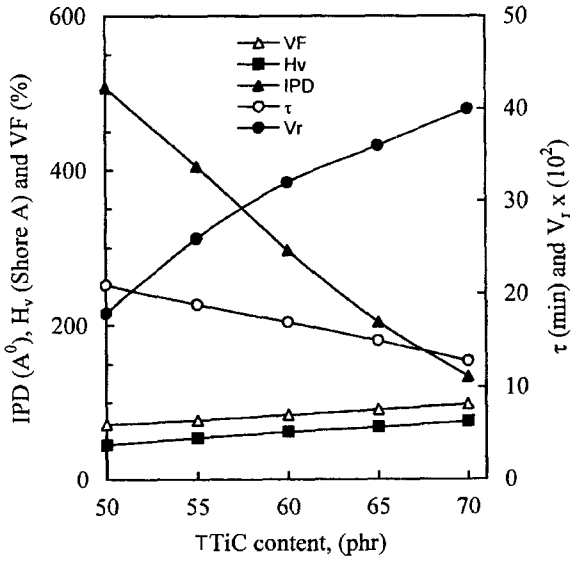

Figure 2. The values of IPD, H_v, VF, V_r and τ against TiC content of SBR composites.

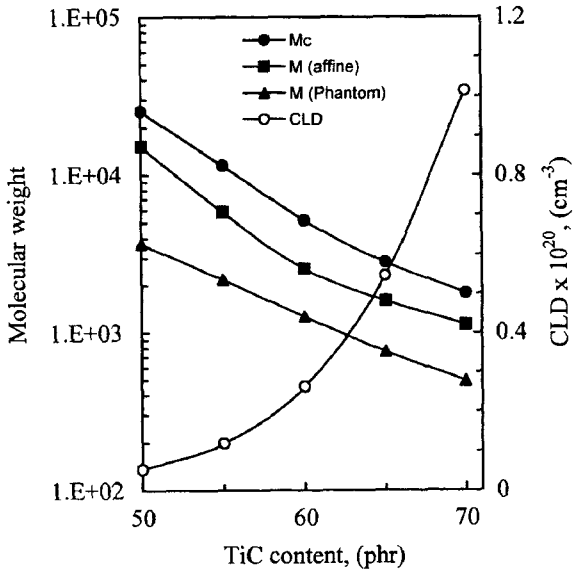

Figure 4. The M_c, M_{affine}, $M_{phantom}$ and CLD against TiC content.

rubber and conductive particles. Thus, TiC has a positive effect in this interaction. The experimental values of M_c are close to the affine network model results. This implies that the crosslinking junctions are embedded in the network and cannot fluctuate freely, and that the chain vector transforms linearly with macroscopic deformation.[25,26] We can therefore speculate that the SBR polymeric composites have modified chain structure and consequently also enhanced the network structure core of rubber matrix as confirmed by SEM analysis. SEM micrographs of SBR-TiC composites for samples (FT0 and FT20) are shown in Figure 5(a, b). At low content of TiC (i.e. sample F0) the conductive particles accumulate in an irregular pattern, a gross phase separation and form cluster aggregates of quasi-globules form as observed in Figure 5(a). While (sample FT20), TiC interacts with SBR polymeric matrix and forms continuous network morphology structures as seen in Figure 5(b). This continuous network structure provides composites with conducting paths and/or channels. Therefore the continuous channels and uniforms dispersed of TiC on SBR polymeric matrix took the advantage of the electrical and thermal properties of SBR polymeric composites in an efficient way.

Insulator-Conductor Transition. The conductivity values at room temperature about 20 °C versus TiC content are presented in Figure 6. It is seen that with only ≤ 50 parts per hundred resin(phr) of conductive particle content the material changed from an insulator to conductor composites with a conductivity of 2.24×10^{-6} (Ohm · cm)$^{-1}$. There is a sudden increase in conductivity at 40 phr of conductive particles. This concentration is known as the critical concentration (ϕ_c) of conductive particles and represents about 32.7% according to the values in Table I. This implies that the sudden increase of conductivity accurse at when the volume fraction of conductive particles in the composites exceeds 32.7%. The percolation threshold (P_s) for these composites is 0.327. The high value of P_s in the present composites can be explained by a good homogeneous distribution of conductive phases forming wide paths in SBR matrix as confirmed above.

The Filling factor (F_F) of conductive particles is related to the percolation threshold (P_s) by the following equation:[28]

$$F_F = \left(\frac{\phi_c}{P_s}\right) \text{ and } P_s = \left(\frac{3F_F}{2Z_{eff}}\right) \quad (15)$$

where Z_{eff} is the effective coordination number.

The estimated value of the critical volume fraction ϕ_c corresponding to P_s is 0.336. The calculated value of F_F and Z_{eff} are 0.973 and 4.344, respectively. This means that the conductive particles form network structure in rubber matrix and the percolation of these composites is bond percolation.[28-30]

However, the conductivity-concentration dependence can be explained in terms of percolation theory, which predicts that the conductivity obeys the equation:

$$\sigma = \sigma_1(\phi - \phi_c)^{\vartheta} \quad (16)$$

where σ_1 is a constant and ϕ is the concentration of conduc-

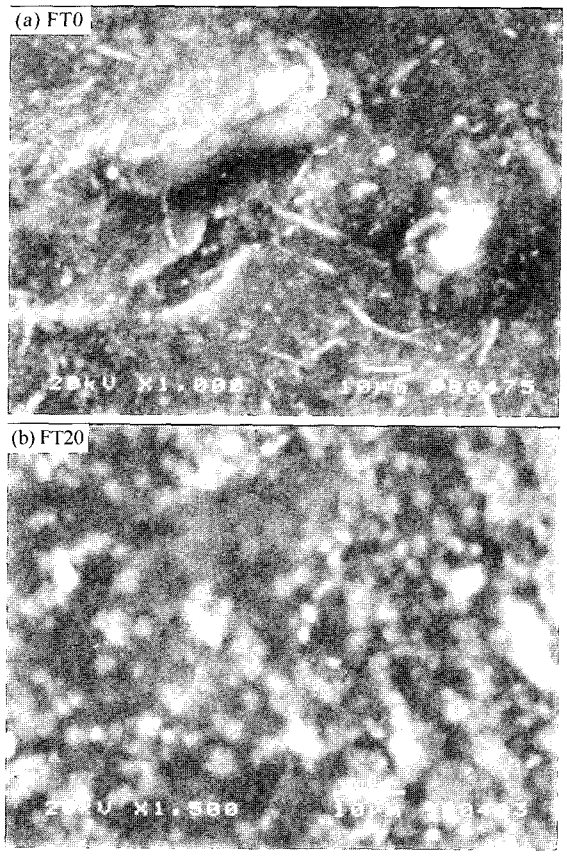

Figure 5. SEM micrograph of SBR/TiC composites for samples, (a) FT0 and (b) FT20.

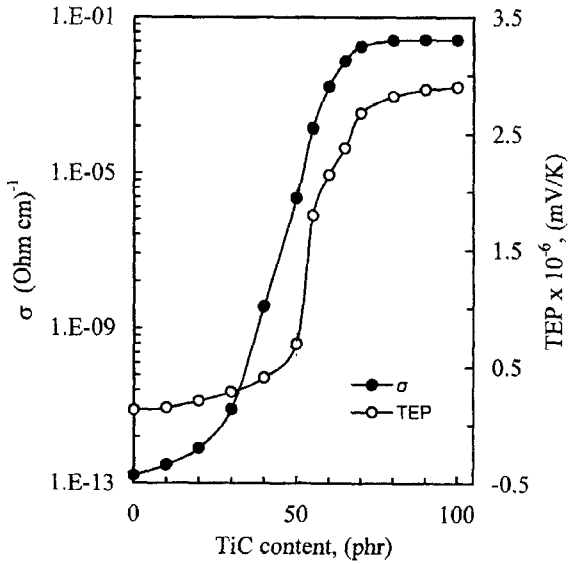

Figure 6. Electrical conductivity and TEP values at room temperature about 20 °C versus TiC content of SBR composites.

tive particles. The value of critical exponent g is about 3.042. As evidence in Figure 6, the TEP above percolation threshold was not dependent on concentration of conductive filler. This also support that the conducting network paths by filled TiC is formed at the concentration higher than the percolation threshold. This result supports that, the increase of TiC content leads not only to a higher number of conducting paths, but also to a larger probability of charge carriers tunneling and/or hopping between the conductive particles. It is noticeable that the TEP of SBR/TiC composites increased linearly as shown in Figure 7. Thereby, the polymeric composite is in the semiconductor state and is the P-type semiconductor.

NTCC and PTCC Transition. Figure 8 illustrates the temperature dependence of the electric conductivity of SBR/TiC polymeric composites. It is clear that the valley-shaped conductivity was shifted towards the higher temperature depending on TiC content. This argument confirms that the TiC improves the molecular architecture structure and thermal stability of rubber matrix as confirmed before. It is also found that at relatively low temperature the conductivity is slightly dependent on temperature. This may be attributed to the direct contact of conductive aggregates, which resists the breakage as the rubber is thermally expanded. At moderate temperatures, the conductivity decreases with temperature. The decreases in the number of the conductive filaments decrease the conductivity significantly. The temperature dependence of conductivity in this range (50-100 °C) can be expressed as:

$$\sigma = \sigma_2 \exp\left(\frac{-E_c}{K_\beta T}\right) \tag{17}$$

where σ_2 is the pre-exponential factor and E_c is the carrier's activation energy. The calculated values of E_c as a function of TiC content are plotted in Figure 9(a). The rise of temperature produces a significant volume expansion, which increases the interparticle distance of conductive filaments and reduces the number of conductive filaments, resulting in lower conductivity of the composites. In more confirmation, the coordination numbers as a function of temperature for samples FT0 and FT20 are depicted in Figure 9(b). It is clear that the coordination number of charge carriers decreases with increasing temperature leads to an increase in the number of defects and opens the Fermi gaps (i.e. large range order between conductive particles) within polymer matrix.[1,2]

At high temperatures the NTCC behavior changes abruptly to PTCC at specific temperature (namely switch temperature, T_s). The conductive particles at T_s have a tendency to agglomerate because of van der Waals forces and the covalent bonds among some particles. The IPD between conductive phasess versus temperature of SBR polymeric composites for samples FT0 and FT20 is shown in Figure 8. It is clear that the IPD increases abruptly close to T_s for both samples, which supports the second suggestion. In case PTCC of region, the thermal activation energy of carriers (E_i) in rubber matrix can be written as:

$$\sigma = \sigma_3 \exp\left(\frac{-E_i}{2K_\beta T}\right) \tag{18}$$

where σ_3 is the pre-exponential factor. The calculated values of E_i versus TiC content are plotted in Figure 9(a). In the case of small polaron hopping, the hopping conductivity is given by

$$\sigma T = \sigma_4 \exp\left(\frac{-E_h}{2K_\beta T}\right) \tag{19}$$

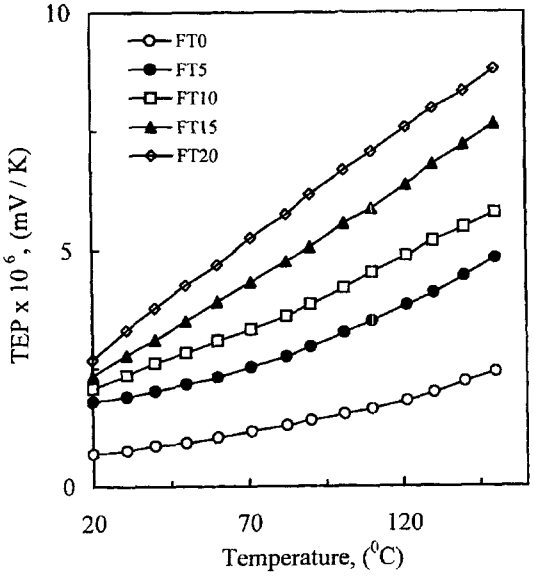

Figure 7. TEP - temperature dependence of SBR/TiC composites.

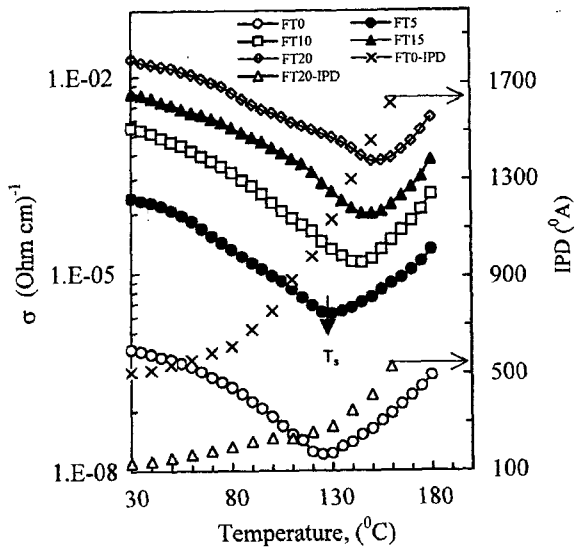

Figure 8. Temperature dependence of the electric conductivity and IPD of SBR composites.

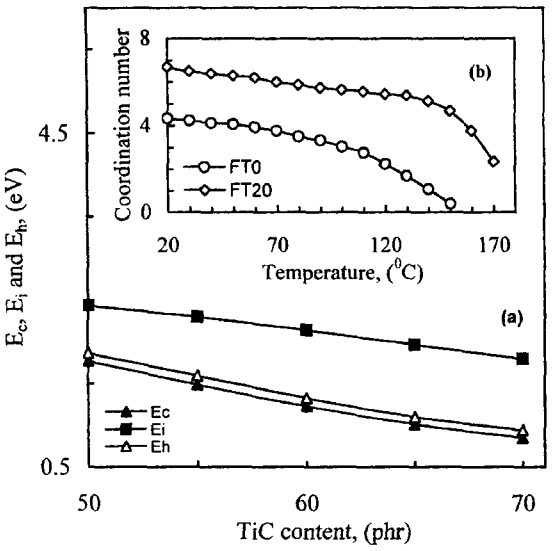

Figure 9. (a) The values of E_c, E_i, E_h versus TiC content and (b) The variation of coordination number with temperature for sample FT0 and FT20.

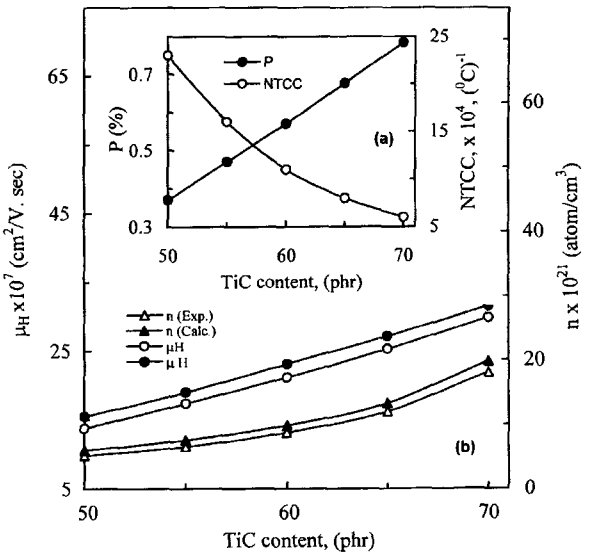

Figure 10. (a) The variation of NTCC and P on TiC content and (b) The calculated and measured values of n and μ_H as a function of TiC content.

where σ_4 is a constant and E_h is the activation energy of hopping. Figure 9(a) shows the calculated values of E_h versus TiC content. From Figure 9(a), it was concluded that the values of E_c are quite close to the E_h. This means that the conduction mechanism of SBR-TiC polymeric composites is governed by a small polaron hopping conduction mechanism.[1,2]

Generally, it is well known that NTCC or PTCC is the one of the important parameters governing the variation of conductivity with temperature. The NTCC or PTCC can be estimated according to the equation.[1,2,31]

$$(NTCC) = \pm\left(\frac{1}{\sigma}\right)\left(\frac{d\sigma}{dT}\right) \tag{20}$$

The performance (P) of SBR polymeric composites as thermistors is determined as[1,2,27]

$$P = \frac{I_{PTCC}}{I_{NTCC}} \tag{21}$$

where I_{NTCC} is the NTCC intensity quantitatively and is defined as[26,31]

$$I_{NTCC} = \log\left(\frac{\sigma_{T_s}}{\sigma_s}\right) \tag{22}$$

where σ_{TS} and σ_s are conductivities at T_s and at room temperature, respectively, and I_{PTCC} is the PTCC intensity quantitatively and is defined as

$$I_{PTCC} = \log\left(\frac{\sigma_{T_s}}{\sigma_T}\right) \tag{23}$$

where σ_T is the conductivity of SBR polymeric composites above T_s and depends on TiC content.

Figure 10(a) gives the variation of NTCC and P versus TiC content. It is clear that the NTCC decrease while P increase with TiC content. This support that TiC improves the network structure management (i.e. increases the ordering and/or homogenates of rubber matrix). From the above discussion, it can be concluded that the SBR-TiC polymeric composites are good NTCC thermistors for consumer products as a self-electrical heating device. Finally, it is worthy mentioned that the (σ-T) curve in Figure 8 can be fitted by the following formula:

$$\sigma = \left(\frac{\sigma_6 e^{-\Psi T}}{1 + e^{\Delta(T_s - T)}}\right) \tag{24}$$

where σ_6 is the initial conductivity, Ψ and Δ are constants strongly dependence on TiC content.

Table II records the calculated fitting parameters of SBR polymeric composites. It is seen that the fitting parameters is good with experimental data up to T_s. It is clear that T_s increases while Ψ and Δ decrease with TiC content. This supports that the TiC enhances the stable structure core into rubber matrix and acts as a degradation inhibitor within SBR polymeric matrix.

Number of Charges (n) and Charge Carrier's Mobility (μ_H). In order to calculate some useful electrical parameters such as number of charge carriers and mobility in the case of small polaron hopping conductivity involving the fixed number of carriers (a) is given by the following equation:[2,16]

$$a = \pm\frac{K_B}{e}\left[\ln\eta\left(\frac{1-c}{c} + \frac{S}{K_B}\right)\right] \tag{25}$$

Table II. The Calculated Values of Fitting Parameters on the Equation[24]

Samples	(Ohm cm)$^{-1}$	T_s (°C)	ψ (°C^{-1})	Δ (°C^{-1})
FT0	7.08 x 10^{-7}	124.4	0.02274	-0.07928
FT5	1.40 x 10^{-4}	130.8	0.02167	-0.06175
FT10	1.66 x 10^{-3}	141.7	0.02099	-0.06118
FT15	5.60 x 10^{-3}	146.6	0.02013	-0.05945
FT20	1.86 x 10^{-2}	152.4	0.01904	-0.04585

where, e is electron charge, S is a vibrational entropy and η is small enough to be neglected. η is a degeneracy factor ($\eta = 1$) and c is the fraction of aggregate sites which contain the electron and is given by the equation:

$$c = \frac{n}{N} \tag{26}$$

where n is a number of electron per unit volume and N is the number of available aggregate sites per unit volume. Let us consider that the conductive aggregates are divided into cubic cells, each of which contains one conductive aggregates of average volume V. Furthermore, the conductive aggregates are homogeneously distributed. Therefore, there are eight conductive aggregate sites in the cubic unit cell, N is expressed as $N = (8/V)$. From eqs (25) and (26), n is expressed as

$$n = \frac{8}{V}\left(\frac{1}{exp(\pm ae/K_B)+1}\right) \tag{27}$$

Figure 10(b) shows the values of n and μ_H received from experimental and calculated as a function of TiC content. It is seen that the experimental values of n and μ_H are close to the calculated data. The value of n and μ_H increases with increasing TiC content. This is ascribed that TiC promotes the molecular architecture to more expanded chain form and increases the free electron density and acts as a pinning center effect in SBR polymeric composites. This leads to enhancement of inter-particle sites of bulk rubber and responsibility of conductivity increase.

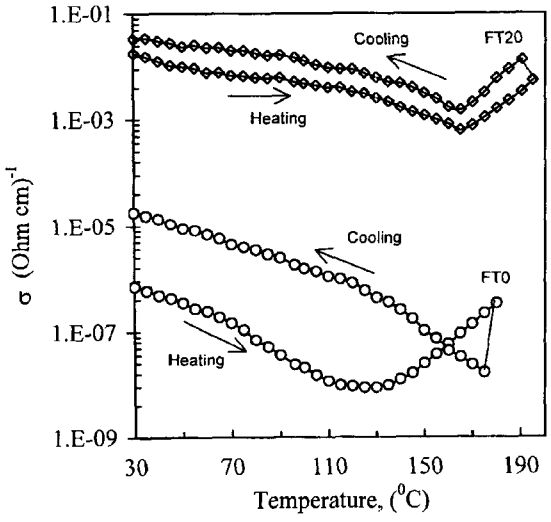

Figure 11. Hesteresis conductivity for samples FT0 and FT20 during the heating and cooling cycles.

Hysteresis Effect. The thermal stability and reproducibility for SBR polymeric composites were investigated by conductivity measurement during heating and cooling cycle. The conductivity versus temperature for samples FT0 and FT20 during the heating and cooling cycles is illustrated in Figure 11. It is observed that the initial and final conductivities at the starting temperature (30 °C) after the heating-cooling cycle are found to be different for both samples. The electrical conductivity set for sample FT0 is much higher in the heating-cooling cycle compared to the sample FT20. This indicates that TiC improves the grain connectivity and orientation of conductive elements. However, the conducting hysteresis for both samples is mainly due to some irreversible change in continuous conducting networks during heating and not completely reversed during cooling. In addition, the hesteresis conductivity indicates that the change of bulk electrical conductivity against temperature is irreversible in nature.

Voltage-Current Characteristics. The I-V experimental results for SBR polymeric composites versus TiC content are plotted in Figure 12(a). It is interesting that the broadening of the I-V characteristics decreases with increasing TiC content, which implies a lowering of the degree of ordering increase with increasing TiC content. According to the results, the behavior of V-I curve can be divided into three stages. First stage; for low values of electric field, the V-I plot is linear (Ohmic), showing a positive slope, indicating Ohmic behavior without any remarkable change of the sample temperature. This may be the interparticle contacts leading to the formation of continuous conductive networks are ensured in the SBR polymeric composites and the current density is controlled by thermal generation electric field across the gap between the continuous conductive networks. Second stage; with increase the electric field the behavior of V-I departures from linear to non-linear (non-Ohmic), this nonlinear is believed to be a drop in electric field strength between the continuous conductive networks with increasing the separation distance due to the unequal thermal expansion of conductive elements and SBR rubber.[1,2,31] Third stage; increasing the electric

field above a certain voltage (namely switch or hot voltage V_s), leads to an increase in the Joule heating effect and consequently increases in the bulk sample temperature and decrease the current that is, shows negative resistance (dI/dV) $\angle$ 0. To explain the phenomena of negative resistance, let us now consider that the electrical operation of conductive particles inside rubber matrix is described by the electric equivalent circuit as shown in Figure 15. We suppose that at high electric field the polymeric matrix contains link and separate conductive particles due to Joule heating effect. Separated conductive particles at high electric field, may have electrostatic capacity, therefore the conductive particles may charge as in the circuit in the Figure 12(b). From the plot, the positive charged conductive particles may generate Coulomb attractive forces among the separated particles and repulsive forces among the linking conductive particles and thus resistance decreases and/or may increase. Thereby, the resistance increases mainly due to a relaxation in pressure at neck surface of the conductive particles and a break in filaments interlinked by conductive particles. In conclusion, negative resistance is clearly generated by Coulomb attractive force at high-applied field in SBR polymeric composites.

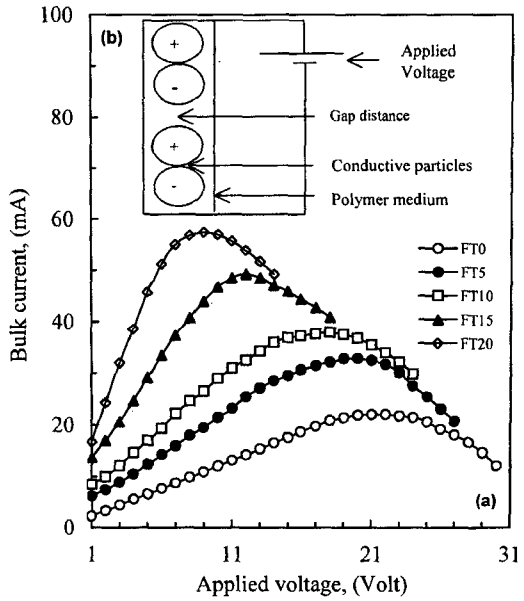

Figure 12. (a) I-V characteristics of SBR composites and (b) the electrical equivalent circuit of conductive particles inside SBR composites.

From the above discussion, it can be said that the SBR-TiC composites are useful for protective and current regulation applications. At the end, I-V curve in Figure 12(a) can be described by the following empirical formula:[20]

$$I = \left(\frac{V}{a \times V^3 + b \times c^{\phi}}\right) \tag{28}$$

where I is the current, V is the applied voltage, $a \times V^3$ and $b \times c^{\phi}$ are resistances which depend on the applied electric field and the dispersion of conductive particles in the polymeric composites.

The fitting parameters of eq (28) are recorded in Table III. It is seen that, the fitting parameters is good with experimental data up to V_s for samples FT0, FT5 and FT10 while quite good for samples FT15 and FT20. The data in Table III indicates that the dispersion of conductive filaments improves with incorporation of TiC.

Working Power-Temperature Behaviors. Figure 13 shows the working power against ultimate temperature of all testes samples. It is clear that the temperature increases with increasing working power and depends on TiC content. It markedly increases the temperature difference produced by Joule heating at the same applied electric power. This evidence indicates that TiC improves the thermal stability of SBR polymeric matrix. In addition, the temperature increase linearly with increasing applied power, this means that our composites can be useful as a temperature sensor.

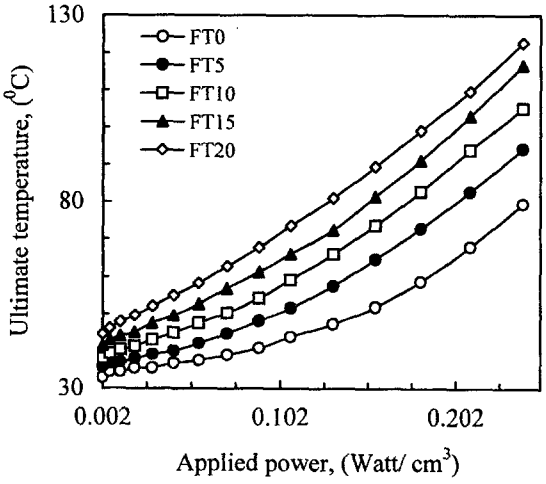

Figure 13. Working power vs. ultimate temperature of all testes samples.

Table III. The Calculated Values of Fitting Parameters of the Equation[28]

Parameters	FT0	FT5	FT10	FT15	FT20
A (Amp) $^{\Omega^{-1}}$	0.02409	0.02351	0.02788	0.04165	0.07439
C	4.77	18.68	17.07	10.58	4.04
b (Ω)	454.5	162.4	117.8	72.7	59.9
ϕ	0.3098	0.3287	0.3466	0.3636	0.3797

1) Time Response to an Applied Power

The temperatureñtime-current(T-t-I) curve of sample FT0 and FT20 during applied electric field about 2 watts for several cycles are shown in Figure 14. It is clear that the optimum and initial temperature change with power cycles and attain to room temperature after several cycles. This may be the power cycles reduced the size of continuous conductive elements and therefore improves the thermal stability of sample FT0. While sample FT20 the temperature time is good stability with power cycles. From these findings it was concluded that TiC improved the thermal stability and reproducibility of microstructure core of rubber matrix under power cycles, which makes them of practical importance to self-electrical heating and automobile applications.

2) Models to computing specific heat and amount of heat transfer

In order to calculate some useful thermal parameters such as the specific heat(C_p) and the amount of heat transferred by radiation and convection(H_r), the bulk temperature due to Joule heating of the rubber samples was recorded as a function of time during the application of electric power across the sample. During measurement the initial applied power was kept constant about 2 Watts up to attaining equilibrium temperature. Then C_p and H_r can be calculated using three models namely: (1) The conservation law of energy, (2) Newton's law of cooling, and (3) Adiabatic model.[1,3,32]

In fact after application of applied voltage on the sample, its temperature T increases with time t and the change dT in time dt is given by the following energy conservation equation:

$$RI^2dt = H_rS(T-T_0)dt + MC_{p(Cons.)}dT \tag{29}$$

where R, M, $C_{p(Cons.)}$ and S are electrical resistance, mass, specific heat and cross section area of the sample respectively, H_r is the amount of heat transfer. The (t-T) curve (Figure 14) shows a thermal growth behavior and after certain time level off (i.e. equilibrium regime). The thermal growth regime can be described by the following empirical formula:

$$\left(\frac{T-T_0}{T_m-T_0}\right) = \left(1-e^{-\frac{t}{\tau_g}}\right) \tag{30}$$

where T_m, and T_0 are the maximum and initial temperatures respectively and τ_g is the thermal growth time constant, depending on TiC content and is determined at $t = \tau_g$. At thermal equilibrium regime (i.e. $dT = 0$) the amount of all heat transfer including heat transfer by radiation and convection are given by:

$$RI^2 = H_rS(T-T_0) \tag{31}$$

The dependence of conduction current on time in Figure 14 can be expressed by:the following equation:

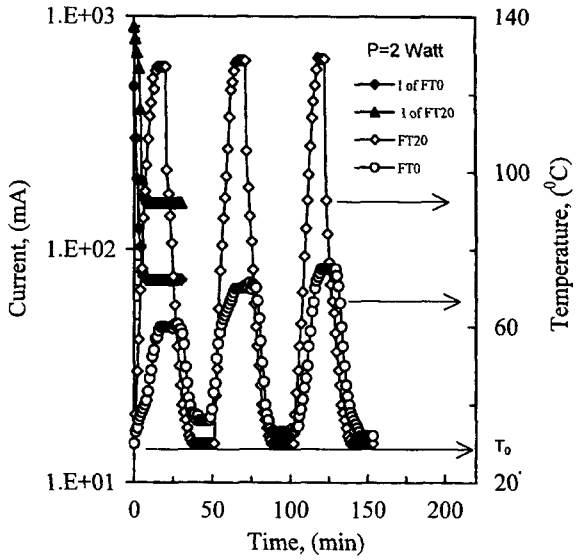

Figure 14. Relationship between temperature, time and current for sample FT0 and FT20 during several thermal cycles i.e. power on about 2 Watt and power off.

$$\left(\frac{I_t-I_0}{I_m-I_0}\right) = \exp-\left(\frac{t}{t_i}\right) \tag{32}$$

where t_i is a decay current constant (in second) and depending on TiC content. From eqs (29)-(31) we get $C_{p(Cons.)}$ as the following:

$$RI^2\int_{t_0}^{t_c} dt = H_rS(T-T_0)\int_{t_0}^{t_c} dt + MC_{p(Cons.)}\int_{T_0}^{T_m} dt \tag{33}$$

By integration eq (31) we get $C_{p(Cons.)}$ in the form:

$$C_{p(Cons.)} = \left(\frac{1}{M(T_m-T_0)}\right)(V_0I_m(T_m-T_0)) + \ln\left(\frac{t_m+t_0}{t_0}\right) + V_0I_mt_m - SH_r(T_m-T_0)\left(t_m-e^{-\frac{t}{\tau_g}}\right) \tag{34}$$

On the other hand, if the thermistor has a uniform temperature during cooling (i.e. power off) the following equation is valid for the cooling of an NTCC in the time interval dt and according to the Newton's law of cooling:

$$-C_{P(Vewt.)}MdT = H_r(T_m-T_0)dt \tag{35}$$

The solution of this equation for any value of t is:

$$(T-T_0) = (T-T_0)\exp(-t/\tau_c) \tag{36}$$

where T_1 is the temperature when the time $t = 0$ and τ_c is the cooling constant in seconds.

From eqs (34),(35) we get $C_{p(Newt.)}$ in the form:

$$C_{p(Newt.)} = \left(\frac{H_r \tau_c}{M}\right)\left(1 - e^{-\frac{t}{\tau_c}}\right) \quad (37)$$

According to the adiabatic model the $C_{p(Adiab.)}$ is given as:[32]

$$C_{p(Adiab.)} = \frac{t_p R I^2}{M(T_m - T_0)} \quad (38)$$

where t_p is the interval time to change the sample temperature from T_0 to T_m.

The calculated and experimental values of C_p and H_r are plotted in Figure 15. The increase of C_p with TiC content is due to the maximizing in network structure (i.e. TiC increases the effective density of SBR composites). It is seen that the calculated and experimental values of C_p are quite agreement. It is interesting that, from the calculated values of H_r per unit sample area per second, one can determine the optimum working conditions to warm a given volume at a given initial boundary condition.

3) Thermal constant

The calculated values of τ_g and τ_c as a function of TiC content for SBR polymeric composites are plotted in Figure 15. It is seen that, τ_g and τ_c decreases with increasing TiC content. This attributed to TiC increases the cross linking density in rubber matrix. This clue reflects that TiC enhances the inner structure of rubber matrix to get more stable thermodynamically.

Thermal Conductivity-Temperature Dependence(λ-T). It is well known that the thermal conductivity value in the polymeric composites depends on the formation of the filler network and the filler loading (i.e. path dependent properties and a bulk properties).[1] Figure 16(a) shows (λ-T) of SBR polymeric composites. It is clear that λ increases with increasing TiC content. This ascribed to TiC maximizing the formation of conductive networks while minimizing the thermal barrier resistance along the heat flow path. It was also observed that, for sample FT0, λ increases gradually up to certain temperature and then gradually decreases with temperature. This is one of evidences that the thermal expansion and free volume of rubber matrix increase with temperature. This leads to an increase the mean widening distance between conductive particles and hence to an increase in the elastic constants related to the intermolecular interaction and/or this may be due to possible crosslinking and degradation effects of SBR polymeric composites. Thus, the thermal gradient will be reduced and so the rate of heat conduction through the sample will be reduced as well the thermal conductivity decreases. While, λ increases linearly with temperature for samples FT5, FT10, FT15 and FT20; this could as a result, thermal barrier resistance along the heat flow path decreases and the packing density increases with TiC content. Further TiC increases the mean free path of phonon and segmental mobility of the polymer molecules. This therefore leads to the increase of λ with temperature. This supports that TiC generates ordering and/or texturing in the microstructure core and modifications in cross-linking density of SBR composites as confirmed by SEM. For the more confirmation of the above idea, let consider λ obeys the percolation law as:

$$\lambda = \lambda_0(\phi - \phi_c)^{\Theta} \quad (39)$$

where λ_0 is a constant and Θ is the critical percolation exponent. Figure 16(b) shows the relation between log λ against log(ϕ - ϕ_c). The calculated value of Θ is about 2.43, which is

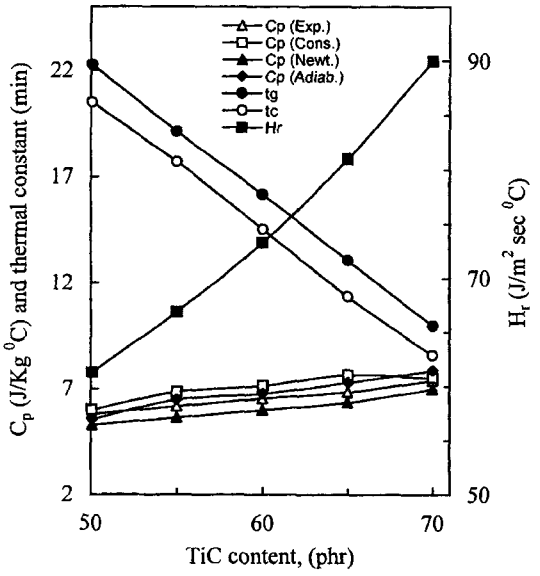

Figure 15. The measured and calculated values of C_p by various models, H_r and thermal constant versus TiC content.

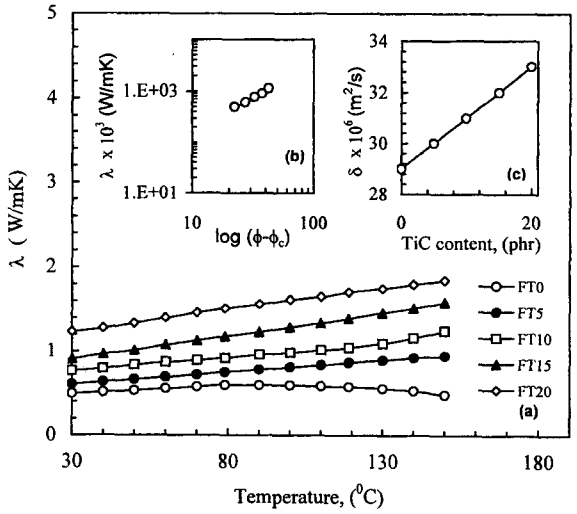

Figure 16. (a) Thermal conductivity versus temperature of SBR/TiC composites, (b) log λ vs. log (ϕ- ϕ_c) thermal, and (c) thermal diffusivity versus TiC content.

in good agreement with the value of 2 in bond percolation. This implies that the TiC maximizes the network structure of rubber matrix.[30] Figure 16(c) shows the relation between δ and TiC content. It is clear that δ increases with increasing TiC content. This attributed to the TiC particles enhance the effective network density into polymeric matrix.

Effective Dielectric Constant-Temperature Dependence. Figure 17 shows the variation of effective dielectric constant-temperature dependence(ε_{eff} - T) for SBR-TiC polymeric composites. The value of ε_{eff} for samples having TiC is higher compared to another one. This may be due to some influence of the vulcanized densities and the effect of TiC on network structure core of rubber matrix. In addition, the number of interfaces increases with increasing volume fraction of conductive particles and the dielectric layer between particles gets thinner. This result leads to an increase of electrical conductivity and permittivity. Also, ε_{eff} increases gradually with temperature without any remarkable change. This may be due to the formation of dipole groups and/or segments that are formed through breakage of chemical bonds during heating and conductive particles combine at random as heterocyclic groups along the main chain during heating. These heterocyclic groups have relatively high moments per one aggregate, which is responsible for the increase of the number of induced dipoles per unit volumes of conductive particles and interfacial polarization.

Electromagnetic Shielding Effectiveness. The electromagnetic wave shielding effectiveness(EMS) can be defined by:[21-24]

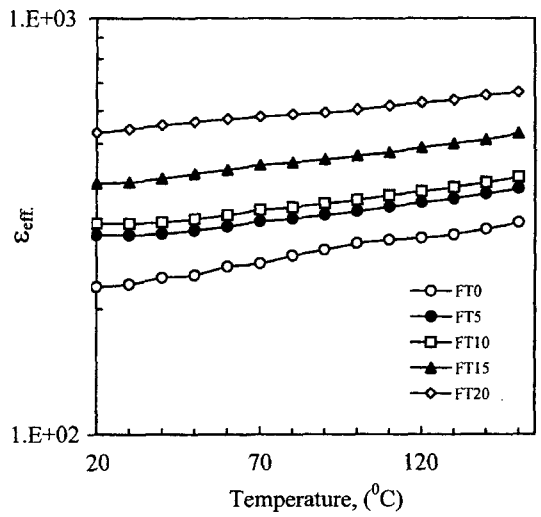

Figure 17. Effective dielectric constant vs. temperature for SBR/TiC composites.

$$EMS = A + R + BdB \tag{40}$$

where A is the absorption loss in dB in the material, due mainly to the conductivity(σ) of the material; R is the reflection loss consisting of the reflections from the material boundaries with the surrounding; and B the successive reflections inside the material, which is negligible in most cases for electrically thick materials. The reflection loss and the absorption loss could be expressed as follows:

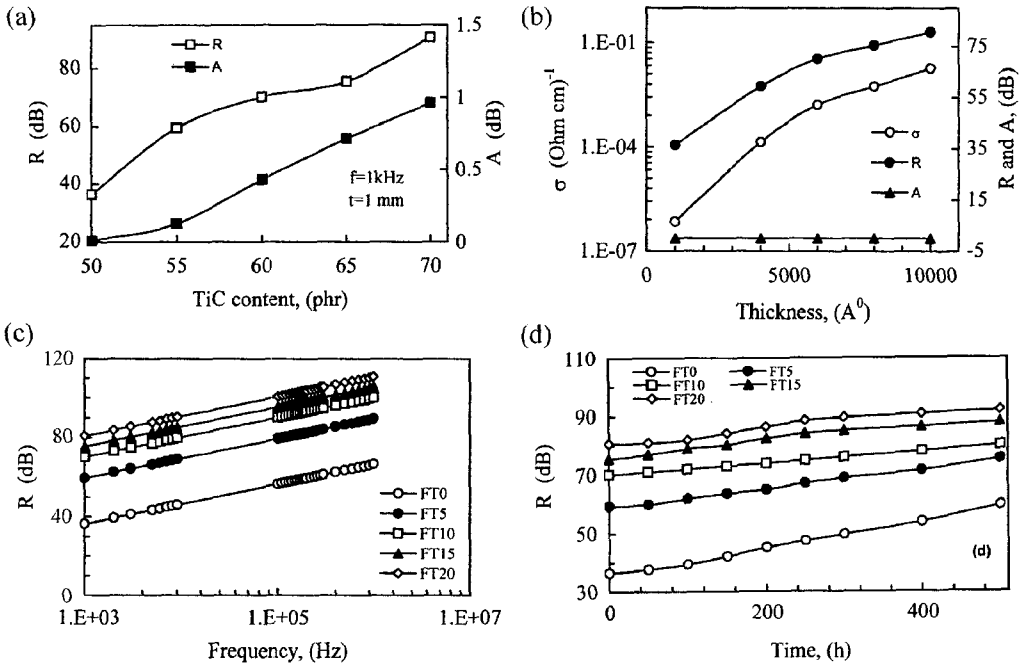

Figure 18. (a) Reflection and absorption loss vs. TiC content, (b) Conductivity, reflection and absorption vs. thickness, (c) Reflection loss vs. frequency, and (d) Reflection loss as a function of annealing time.

$$R = 90.51 + 10\log\left(\frac{f\mu_r}{\sigma}\right) \; dB \tag{41}$$

$$A = 3.35D\sqrt{f\mu_r\sigma} \; dB \tag{42}$$

where f is the frequency, μ_r is the relative permeability and D is the thickness of the sample.

Figure 18(a) shows the variation of R and A on the TiC contents in SBR polymeric composites. It can be said that the absorption coefficient of less than 1 dB was calculated from eq (42) at 1 kHz with film thickness from 0.1 to 1 μm, and the absorption loss is very small compared to the reflection loss. Thereby the electromagnetic wave shielding of SBR-TiC composites can be represented by the reflection loss only. Figure 18(b) shows the dependence of the conductivity, reflection and absorption loss on the thickness of the SBR-TiC polymeric composites. It is clear that the trend of change in reflection loss as a function of SBR film thickness was quite similar to that of conductivity. Figure 18(c) shows the relation between reflection losses versus frequency for SBR polymeric composites containing various content of TiC. The reflection loss of SBR polymeric composites increased with increasing TiC content. This is mainly because of the strong interface between the TiC and the SBR matrix. It has been also believed that, with the increase of TiC content, the gaps between the conductive phases become minimum and the conductive phases become tighter and/or in enough contacts. For this reason, the mobility carriers are easier to hop and/or transfer across gaps into the polymeric matrix.

Annealing Effects. To examine the effect of annealing on the reflection loss of SBR polymeric composites, each sample was annealed in humid chamber at 125 °C for 50, 100, 150, 200 and 250 hrs and then reflection loss was measured. Figure 18(d) shows reflection loss against TiC content with different annealing time. It is clear that the reflection loss increases with the increase of annealing time and depends on the filler content. The results suggested that the crosslinking density (i.e. the link resistance between conductive phases) in the polymeric composites plays an important role. The increase of reflection loss with increasing annealing time can be ascribed to the annealing reduce the residual stress at the filler matrix interface, and finally lead to the stabilization of the contact resistance among conductive phases.

Conclusions

The SBR-TiC polymeric composites have many characteristic properties, which make it suitable for multi applications such as a self-electrical heating, protective, temperature sensor, time delay switching, and electromagnetic wave shielding effectiveness with good thermal stability. The vulcanization reaction depended strongly on the TiC content and network structure of rubber matrix. TiC accelerates the driving force, acts as catalysis, a carrier reservoir during curing process and improves the architecture structure of rubber matrix. Effective concentration of TiC at percolation threshold was about 0.345%. Electron density and mobile carriers increase with increasing TiC content. Thermoelectric power and effective dielectric constant increase linearly with temperature and depend on TiC content. The TEP reveals that the SBR-TiC composite is a p-type semiconductor. In I-V curve, the current increases up to certain voltage depending on TiC content, and then decreases. The decrease in current at high applied electric field may be caused by contacting pressure relaxation and break in conductive particles connectivity induced by Coulomb attractive forces among the separated conductive particles. It has been proved that TiC acts as a stabilizing agent and/or degradation inhibitor, and improves the stability properties of rubber composites. The electromagnetic wave shielding effect is mainly due to the reflection loss and depends on the electrical conductivity and the chain-like structure of the conductive particles in the polymeric matrix.

Acknowledgement. This work was supported by the Dongguk University Research Fund, Seoul, Korea.

References

(1) F. El-Tantawy, *Eur. Polym. J.*, **37**, 565 (2001).
(2) F. El-Tantawy , A. Bakry, and A. R. El-Gohary, *Polym. International*, **49**, 1670 (2000).
(3) H. H. Hassan and E. M. Abdel-Bary, *Appl. Phys. Commun.*, **9**, 267 (1990).
(4) J. Prokes, I. Krivka, and J. Stejskal, *Polym. Deg. Stab.*, **68**, 261 (2000).
(5) Y. Chekanov, R. Ohnogi, S. Asai, and M. Sumita, *Polym. J.*, **30**, 381 (1998).
(6) K. Yoshino, *Jpn. J. Appl. Phys.*, **32**, 979 (1993).
(7) X. H. Yin, *Synthetic Metals*, **69**, 367 (1995).
(8) M. H. Ali and A. Abo-Hashem, *J. Mater. Proc. Tech.*, **68**, 168 (1997).
(9) N. S. Saxena, *Eur. Polym. J.*, **35**, 1687 (1999).
(10) M. M. Badawy, *Polym. Testing*, **15**, 507 (1996).
(11) Y. Fujikura, M. Kawarai, and F. Ozaki, *Polym. J.*, **21**, 609 (1989).
(12) T. G. Gopakumar, *Polym. J.*, **29**, 884 (1997).
(13) W. Hopark, *Polym. J.*, **28**, 672 (1996).
(14) D. Saraydin, *Polym. J.*, **29**, 631 (1997).
(15) J. Shan, *Polym. J.*, **29**, 580 (1997).
(16) M. Okazaki, *Polym. J.*, **31**, 672 (1999).
(17) H. Tagachi, *Physica B*, **270**, 325 (1999).
(18) P. Ghosh and A. Chakrabarti, *Eur. Polym. J.*, **36**, 1043 (2000).
(19) L. Karasek, *Polym. J.*, **28**, 121 (1996).
(20) P. J. Flory, *J. Chem. Phys.*, **18**, 108 (1950).
(21) K. M. Sumita, *J. Mater. Sci.*, **31**, 281 (1996).

(22) N. S. Saxena and P. Pradeep, *Eur. Polym. J.*, **35**, 1687 (1999).
(23) M. Baba, *Polym. Deg. Stab.*, **63**, 121 (1999).
(24) P. S. Majumder, *Radiation Phys. Chem.*, **53**, 63 (1998).
(25) M. C. Chan, *Polym. Eng. Sci.*, **37**, 1127 (1997).
(26) H. Tang, X. Chen, and Y. Luo, *Eur. Polym. J.*, **32**, 963 (1996).
(27) C. Yuksekkalayci, *Polym. Eng. Sci.*, **39**, 1216 (1999).
(28) S. George, *Poymer*, **41**, 579 (2000).
(29) N. Sombatsompop and A. K. Wood, *Polym. Testing*, **16**, 203 (1997).
(30) K. P. Sau, T. K. Chaki, and D. Khastgir, *Polymer*, **39**, 464 (1998).
(31) H. Ishida and S. Rimdusit, *Thermochimica Acta*, **320**, 177 (1998).
(32) H. R. Kokabi, M. Rapeaux, and J. Aymami, *Mater. Sci. Eng.*, **38**, 80 (1996).